International Journal of Mechanical, Industrial and Aerospace Sciences
ISSN: 2517-9950
Vol:4, No:1, 2010

Analysis of Combustion, Performance and Emission Characteristics of Turbocharged LHR Extended Expansion DI Diesel Engine

Mohd.F.Shabir, P. Tamilporai, and B. Rajendra Prasath

***Abstract*—**The fundamental aim of extended expansion concept is to achieve higher work done which in turn leads to higher thermal efficiency. This concept is compatible with the application of turbocharger and LHR engine. The Low Heat Rejection engine was developed by coating the piston crown, cylinder head inside with valves and cylinder liner with partially stabilized zirconia coating of 0.5 mm thickness. Extended expansion in diesel engines is termed as Miller cycle in which the expansion ratio is increased by reducing the compression ratio by modifying the inlet cam for late inlet valve closing. The specific fuel consumption reduces to an appreciable level and the thermal efficiency of the extended expansion turbocharged LHR engine is improved.

In this work, a thermodynamic model was formulated and developed to simulate the LHR based extended expansion turbocharged direct injection diesel engine. It includes a gas flow model, a heat transfer model, and a two zone combustion model. Gas exchange model is modified by incorporating the Miller cycle, by delaying inlet valve closing timing which had resulted in considerable improvement in thermal efficiency of turbocharged LHR engines. The heat transfer model, calculates the convective and radiative heat transfer between the gas and wall by taking into account of the combustion chamber surface temperature swings. Using the two-zone combustion model, the combustion parameters and the chemical equilibrium compositions were determined. The chemical equilibrium compositions were used to calculate the Nitric oxide formation rate by assuming a modified Zeldovich mechanism. The accuracy of this model is scrutinized against actual test results from the engine. The factors which affect thermal efficiency and exhaust emissions were deduced and their influences were discussed. In the final analysis it is seen that there is an excellent agreement in all of these evaluations.

***Keywords*—**Low Heat Rejection, Miller cycle.

I. Introduction

ENERGY conservation and efficiency have always been the quest of engineers concerned with internal combustion engines. The diesel engine generally offers better fuel economy than its counterpart petrol engine. Even the diesel engine rejects about two thirds of heat energy of the fuel, one-third to the coolant, and one third to the exhaust, leaving only about one-third as useful power output. Theoretically if the heat rejected could be reduced, then the thermal efficiency would be improved, at least up to the limit set by the second law of thermodynamics. Low Heat Rejection engines aim to do this by reducing the heat energy from transferring to the engine coolant. This energy could be recovered to promote a slight power increase at the flywheel and at turbocharger with higher boost and higher efficiency. This Low heat rejection (LHR) engine concept proved to be a viable means of recovering thermal energy normally radiated or exhausted from the diesel engine [1].

A Low heat rejection engines employs suitable insulation coatings such as ceramics etc to the cylinder and piston. LHR engine with 0.5 mm thickness insulation coating for components gives better performance than with 1 mm thickness. The thermal efficiency with 0.5 mm coating is higher by about 6 to 8% under various operating conditions [5]. Due to the insulation provided on the required surfaces of the cylinder, the amount of heat loss to the coolant is reduced and hence results in high combustion chamber temperatures. This leads to severe problems such as high NO_x emission levels and exhaust blow-down losses.

The blow-down losses are mainly associated with the difference in pressure between the engine cylinder and turbine inlet duct prevailing at the beginning of the exhaust stroke. This can be overcome by using a concept called expanded cycle [8]. The extended expansion cycle with a short compression stroke is one of the engine concepts that are available for improving engine performance and reducing fuel consumption. The short compression stroke is achieved by late closing of the intake valve [6]. These engines with extended expansion stroke and short compression stroke are also known as Miller cycle. Diesel engines with extended expansion strokes can be expected to have specific fuel consumption up to about 8% lower, than those achievable with conventional diesel engines employing equal compression and expansion strokes [8][9]. For both spark ignition and Diesel engines the use of extended expansion reduces emissions in proportion of specific fuel consumption [9].

Manuscript received November 1, 2009.

Mohd.F.Shabir is with the Department of Mechanical Engineering, Tagore Engineering College, Affiliated to Anna University, Chennai, Tamilnadu, India (phone: 9144-22532327; fax: 9144-27409729; e-mail: ffshabir2001@yahoo.co.in).

P.Tamilporai is with the Internal Combustion Engineering Division, Department of Mechanical Engineering, Anna University, Chennai, Tamilnadu, India (e-mail: tporai@annauniv.edu).

B.Rajendra Prasath is with the Internal Combustion Engineering Division, Department of Mechanical Engineering, Anna University, Chennai, Tamilnadu, India (e-mail: br_prasath@rediffmail.com).

To understand the fundamental processes in engine system the development of computer technology has encouraged the use of simulation models. Hence, computer simulation has been performed for IC engine processes for each degree crank angle using the 'C' language to predict the performance and emissions of the test engine.

A. Low Heat Rejection Engines

The basic means of reducing heat rejection and loss in engines is to insulate the combustion chamber [2]. The primary advantage of low heat rejection engines is the increased gas temperatures that are allowed and maintained during operation. This corresponds to an increased enthalpy in the exhaust gases. Progress in raising combustion temperatures in the early days of engine design was restricted by the limitations of cast irons and other construction materials. Thick walled combustion chambers were built to conduct heat away from the burning gases in the cylinder. Materials that were then examined included glass derivatives and others thought to have low thermal conductivities. Glass had excellent insulating qualities, low expansion ratios, low cost, but unfortunately lacks sufficient strength for engines. The desirable material characteristics are Low thermal conductivity, Low specific heat, High flexure strength, High fracture toughness, High thermal shock resistance, Good wear resistance, Chemical inertness and Thermal expansion equal to iron and steel.

Zirconia is a ceramic material that has very low thermal conductivity values, good strength, thermal expansion coefficients similar to metals, and is able to withstand much higher temperatures than metals. However, one disadvantageous trait is its characteristic of changing phases as its temperature is greatly increased. Phase changes occur on the molecular level and involve the altering of molecular bonding and structure. Eliminating this phase change would ease the burdens of construction and use of the material in an engine that would often go through the problem temperature ranges. Partially stabilized zirconia (PSZ) has been developed that decreases the magnitudes of these changes and is now considered a good candidate for engine use [2].

In this case, the turbocharged conventional engine is modified to turbocharged LHR engine by insulating the combustion chamber surfaces and coolant side of the cylinder with partially stabilized zirconia of 0.5 mm thickness. Insulated engine components consist of pistons, cylinder head with valves and cylinder liner. Fig.1 shows the photographic view of engine components before ceramic coating and Fig.2 to 4 shows the Photographic view of engine components like cylinder liner, piston top and cylinder head with valves after ceramic coating respectively.

Fig. 1 Photographic View of Engine Components (Before Coating)

Fig. 2 Photographic View of Cylinder Liner (After Ceramic Coating)

Fig. 3 Photographic View of Piston top (After Ceramic Coating)

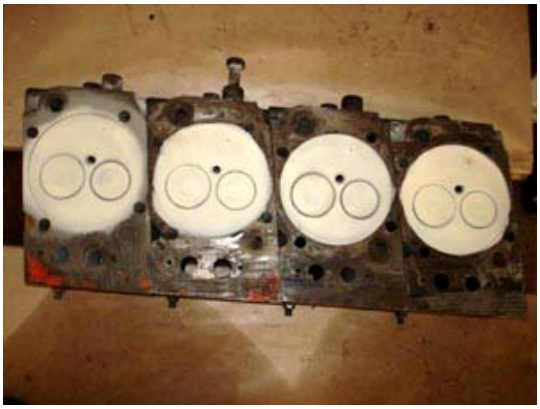

Fig. 4 Photographic View of Cylinder Head with valves (After Ceramic Coating)

B. Extended Expansion (Or) Miller Cycle

The Extended expansion or Miller cycle concept was achieved, in this case by closing the inlet valve late. Conventionally, the inlet valve closes at 45º aBDC. In the Miller cycle the inlet valve is allowed to close at 60ºaBDC. Fig.5 and 6 shows the conventional valve timing diagram and extended expansion cycle valve timing diagram respectively.

The valve timing diagram was modified by modifying the intake cam. Fig.7 and 8 shows the conventional intake cam and the modified intake cam respectively. The duration of inlet valve opening in the conventional valve timing diagram is 233º Crank angle (CA) and in the case of the extended expansion cycle is 248º Crank angle (CA).

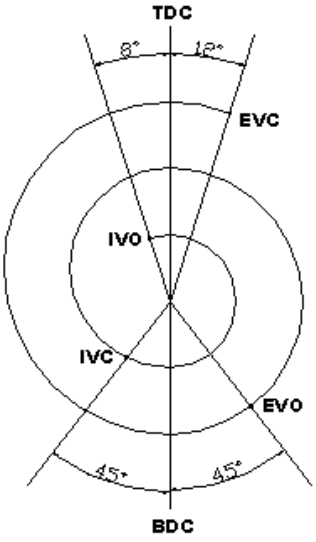

Fig. 5 Conventional valve timing diagram

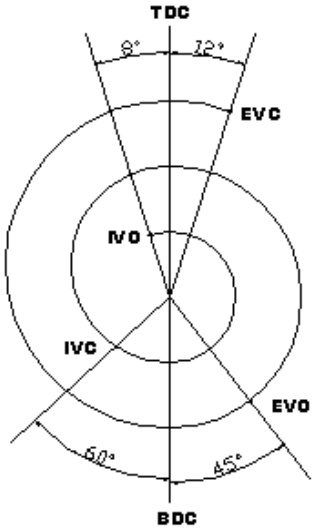

Fig. 6 Extended expansion cycle valve timing diagram

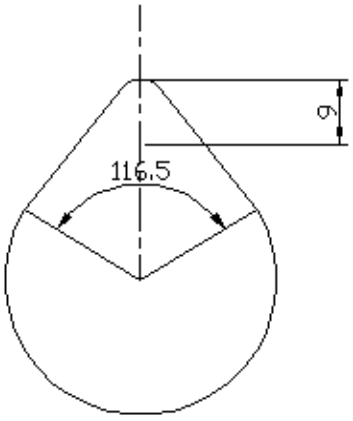

Fig. 7 Conventional intake cam

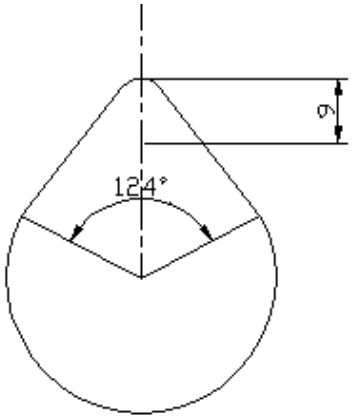

Fig. 8 Modified intake cam

II. Simulation Procedure

Calculation of Number of Moles of Species of Reactant and Product

In this simulation during the start of compression, the mole of different species that are considered to be present includes oxygen, nitrogen from intake and carbon dioxide, water (gaseous), nitrogen and oxygen from the residual gases. The overall complete combustion equation considered is

$$C_nH_m + \lambda\left(n+\frac{m}{4}\right)\left(O_2 + 3.773 * N_2\right) \rightarrow nCO_2 + \left(\frac{m}{2}\right) * H_2O + 3.773 * \left(n+\frac{m}{4}\right) * N_2 + (\lambda - 1)\left(n+\frac{m}{4}\right)O_2 \quad (1)$$

λ excess air ratio
n Number of carbon atoms in diesel
m Number of hydrogen atoms in diesel

Total Moles of Species of Reactant (TMR)

This equation gives total number of moles of species of reactant

$$TMR = 1 + \lambda\left(n+\frac{m}{4}\right) * 4.773 \quad (2)$$

Total Moles of Species of Product (TMP)

This equation gives total number of moles of species of product

$$TMP = 4.773 * n + 1.443 * m + (\lambda - 1) * \left(n+\frac{m}{4}\right) \quad (3)$$

Cylinder Volume (V_θ)

Cylinder volume at a crank angle is calculated from the equation given by [16]

$$V_\theta = V_C + \left(\pi * \frac{B^2}{4} * \frac{S}{2}\right)\left(1 + z - \left(z^2 - \sin^2\theta\right)^{\frac{1}{2}} - \cos\theta\right) \quad (4)$$

$$z = \frac{l_C}{\left(\frac{S}{2}\right)} \quad (5)$$

V_C Cylinder volume (m^3)
B Bore diameter (m)
S Stroke length (m)
l_C Connecting rod length (m)
z Constant

Initial Temperature and Pressure during Start of Compression

Initial temperature at the beginning of the compression process is calculated as follows [16]

$$T_2 = T_1 * \left(\frac{V_1}{V_2}\right)^{\frac{R}{C_V(T_1)}} \quad (6)$$

$$P_2 = \left(\frac{V_1}{V_2}\right) * \left(\frac{T_2}{T_1}\right) * P_1 \quad (7)$$

T Cylinder Temperature (K)
P Cylinder Pressure (bar)
V Cylinder volume (m^3)
R Characterestic gas constant (kJ/kg-K)
C_V Specific heat at constant volume (kJ/kg-K)

Work Done (dW)

Work done in each crank angle

$$dW = \left(\frac{P_1 + P_2}{2}\right)(V_2 - V_1) \quad (8)$$

Mass of Fuel Injected

Considering that nozzle open area is constant during the injection period, mass of the fuel injected for each crank angle is calculated using the following expression given by [4]

$$m_f = C_D A_n \sqrt{2\rho_f \Delta P}\left(\frac{\Delta\theta}{360N}\right) \quad (9)$$

m_f Mass of fuel injected (kg)
C_D Coefficient of discharge of injector nozzle
A_n Nozzle hole area (m^2)
ρ_f Density of fuel (kg/m^3)
ΔP Pressure drop across the nozzle
$\Delta\theta$ Nozzle open period in crank angle degrees
N Engine speed (rpm)

Unburned Zone Temperature

The unburned zone temperature is calculated using the equation given by [31]

$$T_u = T_{SOC}\left(\frac{p}{p_{SOC}}\right)^{\frac{\gamma-1}{\gamma}} \quad (10)$$

T_u Unburned zone temperature (K)
T_{SOC} Temperature during the start of combustion (K)

p_{SOC} Pressure during the start of combustion (bar)

Preparation Rate

The preparation rate is calculated using the following equation given by [16]

$$P_r = KM_i^{(1-x)} M_u^{\ x} P_{O_2}^{\ L} \quad (11)$$

$$K = 0.085N^{0.414} M^{1.414} P_i^{-1.414} h^{-1.414} d_n^{-3.644} \quad (12)$$

P_r Preparation rate (kg per degree crank angle)

P_{O_2} Partial pressure of oxygen (bar)

M_i Total mass of fuel injected in the cylinder upto the time of injection (kg)

M_u Part of the fuel still available for preparation (kg)

M Mass of fuel injected (grams/cycle/cylinder)

K Constant

P_i Injection period (degree crank angle)

h Number of nozzle holes in injector nozzle

d_n Nozzle hole diameter (mm)

L, x Constants

Reaction Rate

The reaction rate is calculated using the following equation given by [16]

$$R_{r(\theta+1)} = \frac{K^1 P_{O2}}{N\sqrt{T}} e^{\frac{-act}{T}} \int (P_{r(\theta+1)} - R_{r(\theta)}) d\theta \quad (13)$$

R_r Reaction rate (kg per degree crank angle)

θ Crank angle (degree)

act Activation energy

K^1 Constant

Initial Temperature

Initial temperature during the start of combustion after the ignition delay is calculated using the equation given below

$$T_2 = T_1 * \left(\frac{V_1}{V_2}\right)^{\frac{R}{C_v(T_1)}} + \frac{dM_f Q_{vs}}{M_1 C_v(T_1)} \quad (14)$$

M_1 Mass in cylinder during start of combustion (kg)

M_f Mass of fuel (kg)

Q_{vs} Lower heating value (kJ/kg)

Annand's Total Heat Transfer Model

First term of this equation shows that Prandtl number for the gases forming the cylinder contents will be approximately constant at a value 0.7, claims that Reynolds number is the major parameter affecting convection. The second is a straight forward radiation term assuming grey body radiation.

$$\frac{dQ}{dt} = ak\frac{\mathrm{Re}^b}{d}(T_C - T_W) + c(T_C^{\ 4} - T_W^4) \quad (15)$$

Q Total Heat transfer (kJ)

a, b, c Constants

Re Reynolds number

T_w Cylinder wall temperature (K)

T_C Cylinder mean temperature (K)

Wall Heat Transfer Model

This model is used to find out conductive heat transfer through cylinder to the coolant and thereby to find instantaneous wall temperature.

Initial temperature is found out using the following expression [5]

$$T_w = T_g - \left(Q_w \Big/ h_g 2\pi r_1 l\right) \quad (16)$$

$$Q_w = \frac{T_g - T_w}{R} \quad (17)$$

Q_w Wall Heat transfer (kJ)

T_g Gas temperature (K)

h_g Gas wall heat transfer coefficient (kJ/m^2–hr–K)

l Stroke length (m)

The total conductive resistance offered by the cylinder liner, piston rings, cylinder head and piston for the heat transfer from cylinder gases to coolant is calculated from the following expression given by [5]

$$R = (1/h_g 2\pi r_1 l) + (1/h_c 2\pi r_3 l) + \log_e(r_2/r_1)/(k_1 2\pi l_1) + \log_e(r_3/r_4)/(k_c 2\pi l_1) + 3\log_e(r_5/r_9)/(k_r 2\pi l_r) + \log_e(r_7/r_8)/(k_s 2\pi l_s) + (T_p/k_p 2\pi r_7^2) \quad (18)$$

R Total conductive resistance

l_1 Cylinder length (m)

T_p Thickness of the piston crown (m)

h_c Wall – coolant heat transfer coefficient (KJ/m^2–hr–K)

k_c Thermal conductivity of ceramic material (W/m^2-K)

k_s Thermal conductivity of skirt material (W/m^2-K)

k_l Thermal conductivity of liner material (W/m^2-K)

k_p Thermal conductivity of piston material (W/m^2-K)

k_r Thermal conductivity of ring material (W/m^2-K)

$r_1, r_2, r_3, r_4, r_5, r_7, r_8, r_9$ Radii of the composite cylinder wall with respect to cylinder axis (m)

Energy Equation

According to first law of thermodynamics the energy balance equation is given by

$$E(T_2) = E(T_1) - dW - dQ + dM_f Q_{VS} \quad (19)$$

E Internal energy (kJ)

ER Error in accuracy

M_2 Mass in the cylinder at the end of combustion

To find the correct value of T_2, both sides of the above equation should be balanced.

So the above equation is rearranged as shown below

$$ER = E(T_2) - E(T_1) + dW + dQ - dM_f Q_{VS} \quad (20)$$

If the numerical value of ER is less than the accuracy required, then the correct value of T_2 has been established, otherwise a new value of T_2 is calculated for new internal energy and C_v values.

$$ER^1 = C_V(T_2) * M_2 \quad (21)$$

$$(T_2)_n = (T_2)_{n-1} - \frac{ER}{ER'} \quad (22)$$

Nitric Oxide Formation

Initial nitric oxide formation rate is given by [4]

$$\frac{d[NO]}{dt} = \frac{6*10^{16}}{\sqrt{T}} \exp\left(\frac{-69090}{T}\right)[O_2]_e^{1/2}[N_2]_e \quad (23)$$

$$\frac{d[NO]}{dt} = \frac{2R_1\{1-([NO]/[NO]_e)^2\}}{1+([NO]/[NO]_e)R_1/(R_2+R_3)} \quad (24)$$

Nitric oxide equilibrium concentrations are calculated by

$$[NO]_e = \left(20.3*\exp(-21650/T)[O_2]_e[N_2]_e\right)^{1/2} \quad (25)$$

[ ] denotes species concentration (moles/cm^3)

$[O_2]_e$ Equilibrium oxygen concentration (moles/cm^3)

$[N_2]_e$ Equilibrium nitrogen concentration (moles/cm^3)

$[NO]$ Nitric oxide concentration (moles/cm^3)

$[NO]_e$ Equilibrium nitrogen oxide concentration (moles/cm^3)

R_1, R_2, R_3 are constants

Minimum Valve Flow Area

The instantaneous flow area depends on valve lift and the geometric details of the valve head, seat and stem. There are three separate stages to the flow area development as valve lift increases. The stages change according to the conditions as the valve lift increases [16].

In the first stage,

$$\frac{w}{\sin\beta\cos\beta} > L_v \quad (26)$$

The minimum flow area is

$$A_m = \pi L_v \cos\beta\left(D_v - 2w + \frac{L_v}{2}\sin\beta\right) \quad (27)$$

In second stage,

$$L_v = \frac{w}{\sin\beta\cos\beta} \quad (28)$$

the minimum flow area is

$$A_m = \pi D_m\left[(L_v - w\tan\beta)^2 + w^2\right]^{\frac{1}{2}} + w\tan\beta \quad (29)$$

$$D_m = D_v - w \quad (30)$$

In the third stage,

$$L_v > \left[\left(\frac{D_p^2 - D_s^2}{4D_m}\right)^2 - w^2\right]^{\frac{1}{2}} + w\tan\beta \quad (31)$$

The minimum flow area is

$$A_m = \frac{\pi}{4}\left(D_p^2 - D_s^2\right) \quad (32)$$

L_v Valve Lift (m)

w Valve seat width (m)

β Valve seat angle (deg)

A_m Minimum flow area (m^2)

D_v Valve head diameter (m)

D_p Port diameter (m)

D_s Valve stem diameter (m)

Mass Flow during Exhaust Blow Down

During exhaust blow-down the flow of gases out of the cylinder is due to high pressure existing within the cylinder. Mass flow rate is given by [16]

$$\frac{dm}{dt} = A_m\sqrt{2\rho dp} \tag{33}$$

ρ Density (kg/m^3)

dp Pressure drop across the valve

Mass Flow during Displacement

During displacement cylinder pressure is assumed constant.

$$\frac{dV}{V} = \frac{dm}{m} + \frac{dT}{T} \tag{34}$$

Intake

The instantaneous mass flow through the inlet valve is given by [16]

$$\dot{m} = C_S\sqrt{dP}A_m dt \tag{35}$$

$$C_S = \sqrt{\frac{2P_a}{RT_a}} \tag{36}$$

Pressure drop across the valve during suction is given by [16]

$$\text{dP}=\left(\frac{NS}{(A_m/A_{cy})\Delta\alpha_o}\right)^2\left(\frac{360}{C_S}\rho_a\right) \tag{37}$$

$\Delta\alpha_o$ Angle of opening (degree)

A_{cy} Cylinder cross-sectional area (m^2)

III. Experimental Set up and Procedure

To validate computer simulation results, cylinder peak pressure was determined through the experiments at identical design and operating conditions. An experiment set-up was developed to conduct test on a four cylinder, four stroke water cooled turbocharged DI Diesel engine. The test engine is coupled with a hydraulic dynamometer. In addition to this, fuel measuring burette, air flow measuring U-tube manometer were also fitted to the test engine set up. A provision was made to mount a piezoelectric pressure transducer flush with the cylinder head surface to measure the cylinder pressure. The engine specifications are number of cylinders 4, cylinder bore 111 mm, stroke 127 mm, rated speed 1500 rpm, compression ratio 16:1, IVO - 8º bTDC, IVC - 45º aBDC, EVO - 45ºbBDC, EVC - 12ºaTDC. The experimental set up is shown in Fig.9. The experiments were carried out on the same engine with modifications to Turbocharged LHR engine by coating the cylinder liner outside, piston top, cylinder head with partially stabilized zirconia of 0.5mm thickness and Turbocharged LHR Extended Expansion engine by late closing of intake valve.

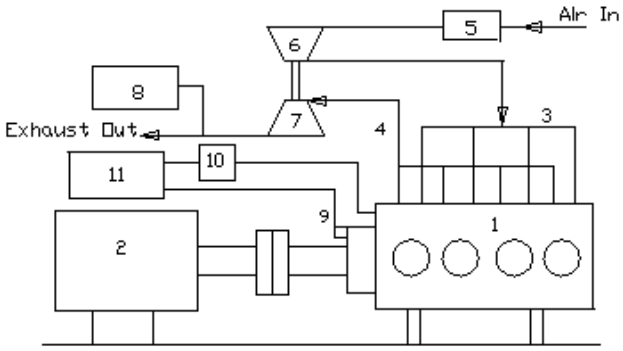

Fig. 9 Experimental Set up

1. Engine
2. Hydraulic dynamometer
3. Inlet line
4. Exhaust line
5. Air surge tank
6. Compressor
7. Turbine
8. Exhaust gas analyzer
9. Crank angle encoder
10. Charge Amplifier
11. CRO

IV. Results and Discussion

Figs. 10-21 shows the comparison of Cylinder Pressure, Cylinder Mean Temperature, Rate of Heat Release, Cumulative Heat Release, Cumulative work done, Total Heat Transfer, Nitric oxide concentration, Brake specific fuel consumption and Brake thermal efficiency for turbocharged conventional engine, turbocharged LHR engine and turbocharged LHR extended expansion engine.

A. Comparison of Cylinder Peak Pressure

Comparison of prediction of in cylinder peak pressure as a function of crank angle is shown in Fig.10. The prediction shows that the cylinder peak pressure for turbocharged LHR engine is higher by about 4.03% and 2.61% when compared to turbocharged conventional and turbocharged LHR extended expansion engine respectively. Under identical conditions the experimental values of cylinder peak pressures as compared to theoretical predictions are higher by 0.52% for turbocharged LHR extended expansion engine and 0.47% for turbocharged conventional engine and 0.17% for turbocharged LHR engine. Fig.11-13 shows the comparison between experimental and simulated values of cylinder pressure for turbocharged conventional, turbocharged LHR and turbocharged LHR extended expansion engine. The increase in the pressure in the case of turbocharged LHR engine is mainly due to higher operating temperature. Also the peak cylinder pressure of

turbocharged LHR extended expansion engine is comparatively lesser than the turbocharged LHR engine because of the lower effective compression ratio.

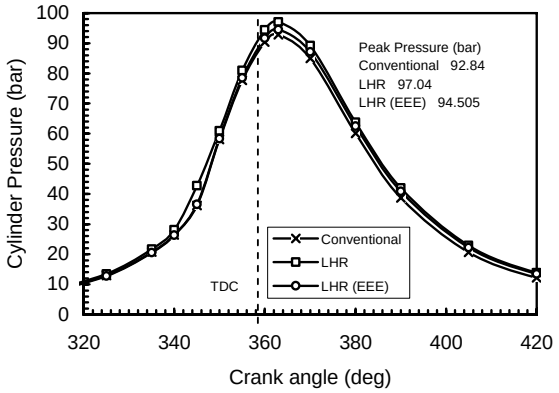

Fig. 10 Comparison of Cylinder Pressure for Conventional, LHR and LHR (EEE) for the diesel fuel supplied (0.0694g/cycle/cylinder) at 1500 rpm

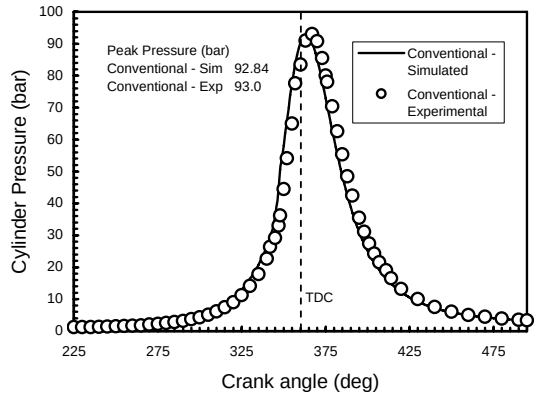

Fig. 11 Comparison of Experimental and Simulated Cylinder Pressure for Turbocharged Conventional engine for the diesel fuel supplied (0.0694g/cycle/cylinder) at 1500 rpm

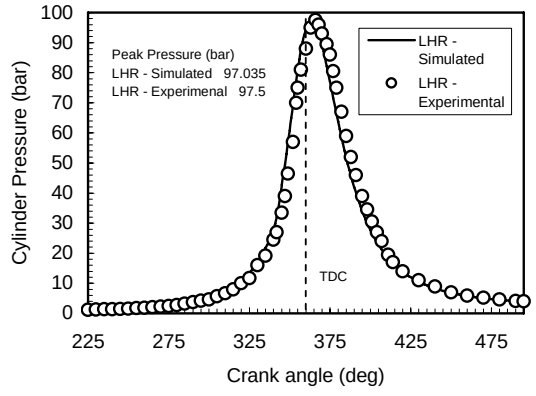

Fig. 12 Comparison of Experimental and Simulated Cylinder Pressure for Turbocharged LHR engine for the diesel fuel supplied (0.0694g/cycle/cylinder) at 1500 rpm

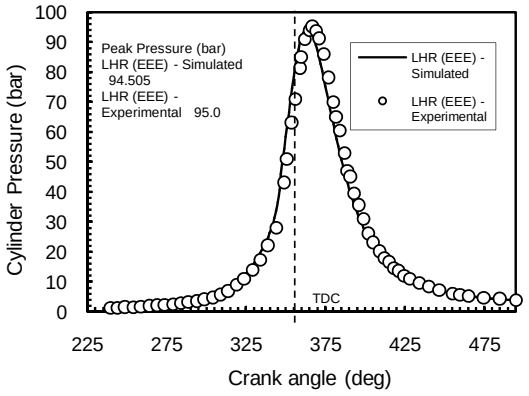

Fig. 13 Comparison of Experimental and Simulated Cylinder Pressure for Turbocharged LHR extended expansion engine for the diesel fuel supplied (0.0694g/cycle/cylinder) at 1500 rpm

B. Comparison of Cylinder Mean Temperature

Fig. 14 shows the comparison of cylinder mean temperature. The percentage increase of cylinder mean peak temperature in the case of turbocharged LHR engine are about 5.69% and 1.45% when compared to turbocharged conventional and turbocharged LHR extended expansion engines. The trend shows that the turbocharged LHR engines are operating at higher temperatures. The high temperatures achieved are mainly attributed to insulation coatings applied to combustion chamber walls.

C. Comparison of Rate of Heat Release

Fig. 15 shows the trend of rate of heat release. The percentage increase in the peak rate of heat release during premixed combustion in the case of turbocharged LHR extended expansion engines were about 25.25% when compared to turbocharged LHR engines and decreased by about 12.42% when compared to turbocharged conventional engine. The trend shows that the turbocharged LHR engines are exhibiting a lower rate of peak heat release during premixed combustion. The decrease in peak heat release during premixed combustion in the case of turbocharged LHR engines is due to the decrease in delay period because of the higher operating temperatures.

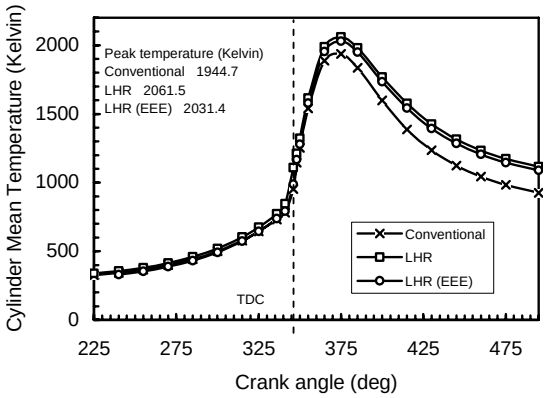

Fig. 14 Comparison of Cylinder Mean Temperature for Conventional, LHR and LHR (EEE) for the diesel fuel supplied (0.0694 g/cycle/cylinder) at 1500 rpm

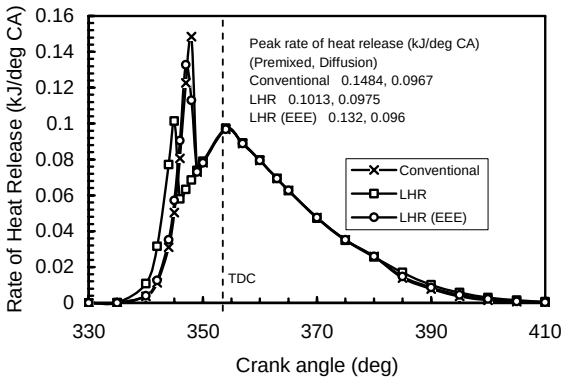

Fig. 15 Comparison of Rate of Heat Release for Conventional, LHR and LHR (EEE) for the diesel fuel supplied (0.0694g/cycle/cylinder) at 1500 rpm

D. Comparison of Cumulative Heat Release

Fig. 16 shows the comparison of cumulative heat release. The percentage increase in cumulative heat release in the case of turbocharged LHR engine are about 2.93% and 1.83% when compared to turbocharged conventional and turbocharged LHR extended expansion engine respectively. The increase in the cumulative heat release in the case of turbocharged LHR engine is due to longer combustion duration due to higher operating temperatures.

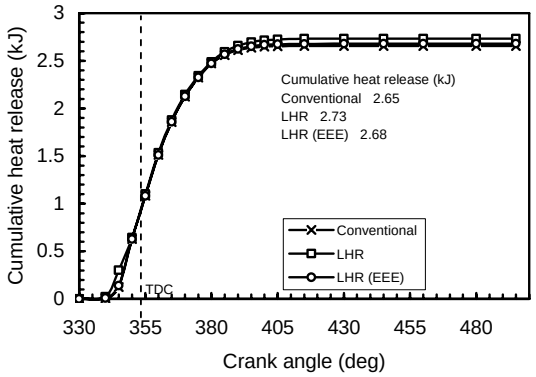

Fig. 16 Comparison of Cumulative heat release for Conventional, LHR and LHR (EEE) for the diesel fuel supplied (0.0694 g/cycle/cylinder) at 1500 rpm

E. Comparison of Cumulative Work Done

The comparison of cumulative work done is shown in Fig.17. The percentage increase in cumulative work done in the case of turbocharged LHR extended expansion engine are about 5.52% and 0.4% when compared to turbocharged conventional and turbocharged LHR engines. This increase in the cumulative work done in the case of turbocharged LHR extended expansion engine is mainly attributed to the decrease in compression work.

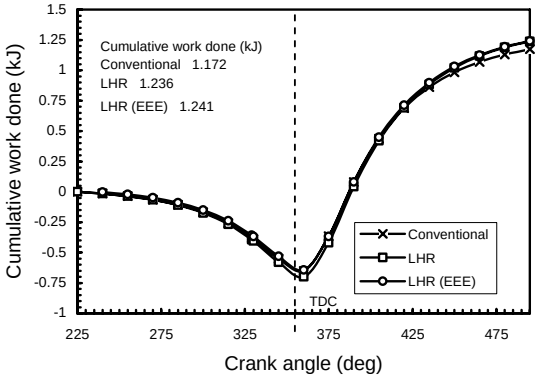

Fig. 17 Comparison of Cumulative work done for Conventional, LHR and LHR (EEE) for the diesel fuel supplied (0.0694g/cycle/cylinder) at 1500 rpm

F. Comparison of Total Heat Transfer

Total heat transfer is the sum of convective and radiative heat transfer. The comparison of total heat transfer is shown in Fig. 18. In the case of turbocharged conventional engines the total heat transfer is higher by about 48.4% and 50.9% when compared to turbocharged LHR and turbocharged LHR extended expansion engine. This is because of the insulation coating applied on the cylinder components. Also it is seen that the total heat transfer in the case of turbocharged LHR extended expansion engines is less then 4.98% when compared

to turbocharged LHR engines, this may be because of the reduced cylinder temperature in the turbocharged LHR extended expansion engine.

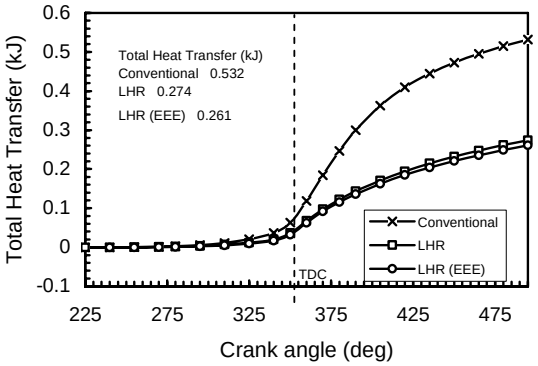

Fig. 18 Comparison of Total heat transfer for Conventional, LHR and LHR (EEE) for the diesel fuel supplied (0.0694g/cycle/cylinder) at 1500 rpm

G. Comparison of Nitric Oxide Concentration

Fig. 19 shows the trend of nitric oxide concentration. The percentage increase in the nitric oxide concentration in the case of turbocharged LHR engines are about 34.45% and 10.6% compared to turbocharged conventional and turbocharged LHR extended expansion engine. The trend shows that the turbocharged LHR engines are producing higher nitric oxide concentration. The increase in nitric oxide concentration in the case of turbocharged LHR engines is because of the higher cylinder mean peak temperature. The decrease in nitric oxide concentration in the case of turbocharged LHR extended expansion engines when compared to turbocharged LHR engine is due to its lower operating temperature because of its lower effective compression ratio.

H. Comparison of Brake Specific Fuel Consumption

Fig. 20 shows the comparison of simulated and experimental brake specific fuel consumption under identical conditions for turbocharged conventional, turbocharged LHR and turbocharged LHR extended expansion engine. For the turbocharged LHR extended expansion, the decrease in brake specific fuel consumption of 3.73%, 3.65%, 3.9%, 3.35% 3.09% and 4.16% at 1000 rpm, 1100 rpm, 1200 rpm, 1300 rpm, 1400 rpm, 1500 rpm speed respectively as compared to that of turbocharged LHR engine are predicted by simulation. Under identical conditions the experimental values are 4.57%, 4.58%, 4.56%, 3.70%, 3.61% and 4.09%.

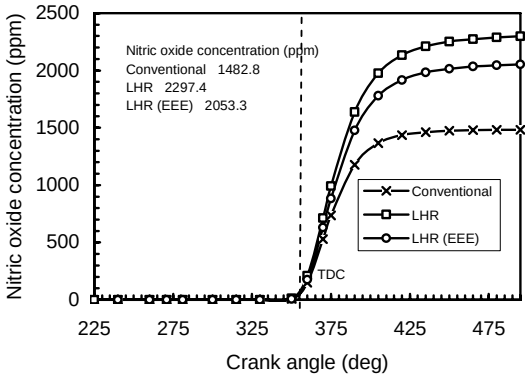

Fig. 19 Comparison of Nitric oxide concentration for Conventional, LHR and LHR (EEE) for the diesel fuel supplied (0.0694g/cycle/cylinder) at 1500 rpm

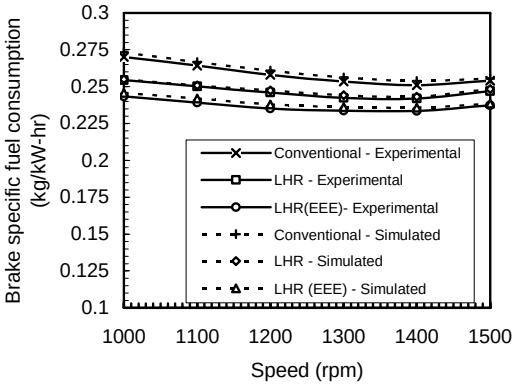

Fig. 20 Comparison of simulated and experimental brake specific fuel consumption for Conventional, LHR and LHR (EEE) for the diesel fuel (0.0694g/cycle/cylinder)

I. Comparison of Brake Thermal Efficiency

Fig. 21 shows the comparison of simulated and experimental brake thermal efficiency under identical conditions for turbocharged conventional, turbocharged LHR and turbocharged LHR extended expansion engine. For the turbocharged LHR extended expansion, the increase in brake thermal efficiency of 3.60%, 3.52%, 3.76%, 3.24%, 3.00% and 3.99% at 1000 rpm, 1100 rpm, 1200 rpm, 1300 rpm, 1400 rpm and 1500 rpm speed respectively as compared to that of turbocharged LHR engine are predicted by simulation. Under identical conditions the experimental values are of 4.37%, 4.38%, 4.36% 3.57%, 3.48% and 3.93%.

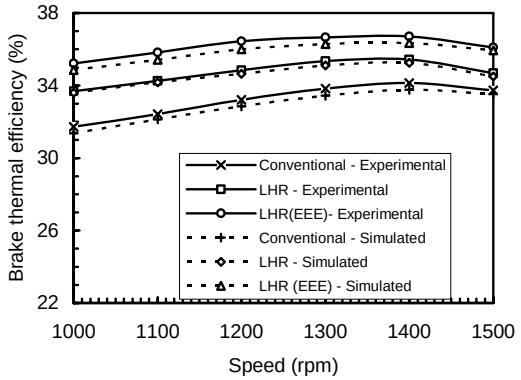

Fig. 21 Comparison of simulated and experimental brake thermal efficiency for Conventional, LHR and LHR (EEE) for the diesel fuel (0.0694g/cycle/cylinder)

V. Conclusion

The turbocharged conventional diesel engine was converted into turbocharged LHR engine and later modified into turbocharged LHR extended expansion engine. The following can be concluded from the data presented.

The increase in the thermal efficiency of Turbocharged LHR extended expansion engine is mainly attributed to the increase in cumulative work done, which may be due to the decrease in work consumed during compression.

The turbocharged LHR extended expansion engine offers superior brake specific fuel consumption over the turbocharged LHR diesel engine.

The turbocharged LHR extended expansion engine shows better lower NOx emission than the turbocharged LHR diesel engine at all speeds and load condition.

Power increase of 4.84% at the rated speed 1500 rpm was achieved at about same fuel consumed for turbocharged LHR extended expansion engine when compared to turbocharged LHR engine.

The simulated results of brake specific fuel consumption and thermal efficiency for the turbocharged conventional engine, turbocharged LHR engine and turbocharged LHR extended expansion engine have been found in good agreement with the experimental results.

Even though this performance is appreciable, still there exists a scope for further improvement to bring the NOx emission level nearer to the practical and useful values of conventionally water cooled engines. This can be done by incorporating both Miller cycle and internal exhaust gas recirculation.

Acknowledgment

Mohd.F.Shabir wish to place on record my deep sense of gratitude and sincere thanks to Professor Dr.P.Tamilporai, Professor and Head, Internal Combustion Engineering Division, Department of Mechanical Engineering, College of Engineering, Guindy, Anna University, Chennai, Tamilnadu, India for his guidance, keen interest and encouragement at every stage of this work. I gratefully acknowledge his kindness, patience and understanding towards me.

Mohd.F.Shabir sincerely thanks Professor Dr.P.Mannar Jawahar, Vice-Chancellor, Anna University for his help and the facilities extended to me to carry out this work.

Mohd.F.Shabir sincerely thanks Ms.Mala, Chairperson, Tagore Engineering College, Affiliated to Anna University, Chennai, Tamilnadu, India for her support and encouragement to carry out this research work.

References

[1] Dorsaf Saad, Philipe Saad and Lloyd Kamo, "Thermal Barrier Coatings for High Output Turbocharged Diesel Engine," SAE paper 2007-01-1442, 2007.

[2] Randolph.A.Churchill, James E. Smith, Nigel N. Clark, and Richard A. Turton, "Low – Heat Rejection Engines – A Concept Review," SAE paper 880014, 1988.

[3] Edwards S.P., Frankle G.R., Wirbeleit F., Raab A., "The Potential of a Combined Miller Cycle and Internal EGR for Future Heavy Duty Truck Applications," SAE paper 980180, 1998.

[4] Heywood J.B., "Internal Combustion Engine Fundamentals," McGraw Hill Book Co., 1988.

[5] Tamil Porai P., Simulation and Analysis of Combustion and Heat Transfer in Low-Heat-Rejection Diesel Engine Using Two-Zone Combustion Model and Different Heat Transfer Models," SAE paper 2003-01-1067, 2003.

[6] Roy Kamo, Nagesh s.Mavinahally and Lloyd kamo, "Emissions Comparisons of an Insulated Turbocharged Multi-Cylinder Miller Cycle Diesel Engine," SAE paper 980888, 1998.

[7] Nagesh Mavinahally and Roy Kamo, "Insulated Miller Cycle Diesel Engine", SAE paper 961050, 1996.

[8] J.A.C.Kentfield, "Diesel Engines with Extended Expansion Strokes," SAE paper 891866, 1989.

[9] J.A.C.Kentfield, "Extended, and Variable, Stroke Reciprocating Internal Combustion Engines," SAE paper 2002-01-1941, 2002.

[10] Miyairi Y., Computer Simulation of an LHR DI Diesel Engine," SAE paper 880187, 1988.

[11] Thomas Morel, Syed Wahiduzzaman, and Edward F.Fort, "Heat Transfer Experiments in an Insulated Diesel," SAE paper 880186, 1988.

[12] Dennis N.Assanis and Edward Badillo, "Transient Analysis of Piston-Liner Heat Transfer in Low-Heat-Rejection Diesel Engines," SAE paper 880189, 1988.

[13] Michael F.J. Brunt, Kieron C.Platts, " Calculation of Heat Release in Direct Injection Diesel Engines," SAE paper 1999-01-0187, 1999.

[14] Hengqing Liu, N.A. Henein, Walter Bryzik, "Simulation of Diesel Engines Cold-Start," SAE paper 2003-01-0080, 2003.

[15] Andreas Pfeifer and Michael Krueger, Ulrich Gruetering, Dean Tomazic, "U.S.2007 – Which Way to Go? Possible Technical Solutions," SAE paper 2003-01-0770, 2003.

[16] Rowland S.Benson, White House N.D., "Internal Combustion Engine," Pergamon Press Ltd, 1979.

[17] Ganesan V., "Computer Simulation of Compression-Ignition Engine Processes ," Universities Press (India) Limited, 2000.

[18] S.Loganathan,P.Tamilporai,"Simulation of Performance of Direct Injection Diesel Engine Fuelled with Oxygenate Blended Diesel," SAE paper 2007-01-0070, 2007.

[19] J.Benajes, J.R.Serrano, S.Molina, R.Novella.," Potential of Atkinson cycle combined with EGR for pollutant control in a HD diesel engine," Energy Conversion and Management 50 (2009) 174-183.

[20] Yanlin Ge, Lingen Chen, Fengrui Sun, Chih Wu, "Performance of an Atkinson cycle with heat transfer, friction and variable specific-heats of the working fluid," Applied Energy 83 (2006) 1210-1221.

[21] Ekrem Buyukkaya, Tahsin Engin, Muhammet Cerit, "Effects of thermal barrier coating on gas emissions and performance of a LHR engine with different injection timings and valve adjustments," Energy Conversion and Management 47 (2006) 1298–1310.

[22] E.G.Giakoumis, "Cylinder wall insulation effects on the first and second-law balances of a turbocharged diesel engine operating under transient load conditions," Energy Conversion and Management 48 (2007) 2925-2933.
[23] Adnan Parlak, Halit Yasar, Bahri Sahin, "Performance and exhaust emission characteristics of a lower compression ratio LHR Diesel engine." Energy Conversion and Management 44 (2003) 163-175.
[24] S.Jaichandar and P.Tamilporai, "Low Heat Rejection Engines – An Overview," SAE paper 2003-01-0405.
[25] Carl-Anders Hergart, Abdelilah Louki and Norbert Peters, "On the Potential of Low Heat Rejection DI Diesel Engines to Reduce Tail-Pipe Emissions," SAE paper 2005-01-0920.
[26] Adnan Parlak, "The effect of heat transfer on performance of the Diesel cycle and exergy of the exhaust gas stream in a LHR Diesel engine at the optimum injection timing," Energy Conversion and Management 46 (2005) 167-179.
[27] Adnan Parlak, Halit Yasar, Can Hasimoglu, Ahmet Kolip, "The effects of injection timing on NOx emissions of a low heat rejection indirect diesel injection engine," Applied Thermal Engineering 25 (2005) 3042-3052.
[28] Claudia Schubert, Andreas Wimmer and Franz Chmela, "Advanced Heat Transfer Model for CI Engines," SAE paper 2005-01-0695.
[29] C.D.McCartan, P.T.McEntee, R.Fleck and G.P.Blair, D.O.Mackey, "Computer Simulation of the Performance of a 1.9 Litre Direct Injection Diesel Engine," SAE paper 2002-01-0070.
[30] Takemi Chikahisa, Mitsuru Konno, Tadashi Murayama, Takuya Kumagai, "Analysis of NO formation characteristics and its control concepts in diesel engines from NO reaction kinetics," JSAE Reviw 15 (1994) 297-303.
[31] Marcus Klein and Lars Eriksson, "A Specific Heat Ratio Model for Single-Zone Heat Release Models," SAE paper 2004-01-1464.
[32] K-Y Teh, S L Miller, and C F Edwards, "Thermodynamic requirement for maximum internal combustion engine cycle efficiency. Part 1: optimal combustion strategy," International Journal of Engine Research Vol.9.
[33] K-Y Teh, S L Miller, and C F Edwards, "Thermodynamic requirement for maximum internal combustion engine cycle efficiency. Part 2: work extraction and reactant preparation strategies," International Journal of Engine Research Vol.9.

Mohd.F.Shabir was born in Chennai, Tamilnadu, India in the year 13.11.1973. He completed his B.E. (Mechanical Engineering) degree from University of Madras in the year 1995 and completed his M.E. (Internal Combustion Engineering) degree with Distinction from Anna University, Chennai, Tamilnadu, India in the year January 2003 and presently pursuing his Ph.D programme in Anna University, Chennai, Tamilnadu, India under the guidance of Dr.P.Tamilporai in the field of "Simulation and Analysis of Low Heat Rejection Extended Expansion engine with iEGR" from January 2006. He is currently working as Associate Professor, Department of Mechanical Engineering, Tagore Engineering College, Affiliated to Anna University, Chennai, India. He became the Member of Indian Society of Technical Education in the year 2004.

P. Tamilporai received his B.E. degree in Mechanical Engineering from Government Engineering College, Salem and M.E. degree in Automobile Engineering from Madras Institute of Technology, Chennai. He obtained his Ph.D degree from Anna University, Chennai. He is currently working as Professor & Head, Internal Combustion Engineering, Department of Mechanical Engineering, Anna University, Chennai, Tamilnadu, India. He is also the Additional Controller of Examinations, Anna University, Chennai. He has vast experience in teaching and guiding research scholars. His main interest of research is "Low Heat Rejection engines". He has presented number of papers in National and International Conferences and has also published a number of National and International Journals.

B. Rajendra Prasath is currently pursuing research work in Anna University under the guidance of Dr.P.Tamilporai. His main interest of research is "Optimization of Performance of Bio-diesel fuel in Low Heat Rejection Engine".